A-4

FBR 8502

COLLEGE OF ENGINEERING

VPI-E-76-4 March 1976

A Deformation Plasticity Analysis of the

Blunted Crack Tip in Plane Strain

J. J. McGowan, Assistant Professor
C. W. Smith, Professor

VIRGINIA POLYTECHNIC INSTITUTE AND STATE UNIVERSITY

BLACKSBURG, VIRGINIA

College of Engineering
Virginia Polytechnic Institute and State University
Blacksburg, VA 24061

VPI-E-76-4 March 1976

A Deformation Plasticity Analysis of the Blunted Crack Tip in Plane Strain

J. J. McGowan, Assistant Professor
C. W. Smith, Professor

Department of Engineering Science and Mechanics

March 1976

Reporting Period: 1974-1975

Prepared For:

National Science Foundation
Washington, D. C.
Grant No. GK 39922

1. Report No. VPI-E-76-4

2. Government Accession No.

3. Recipient's Catalog No.

4. Title

A DEFORMATION PLASTICITY ANALYSIS OF THE BLUNTED CRACK TIP IN PLANE STRAIN

5. Report Date

March 1976

7. Authors

J. J. McGowan and C. W. Smith

8. Performing Organization Report Number

VPI-E-76-4

9. Performing Organization Name & Address

Department of Engineering Science & Mechanics
Virginia Polytechnic Institute & State University
Blacksburg, Virginia 24061

10. Work Unit No.

VPI-323714-1

11. Contract or Grant No.

GK 39922

12. Sponsoring Agency Name and Address

National Science Foundation
Washington, D. C.

13. Type of Report & Period Covered

1974-1975

16. Abstract

This paper presents a deformation plasticity analysis of the tip region of a blunted crack in plane strain. The power hardening material is incompressible both elastically and plastically, in order to simulate behavior of a stress freezing material above critical temperature. The study represents a full field, finite difference solution to the Mode I problem. Stress and displacement fields surrounding the crack tip are presented. The results of this study indicate that the maximum stress seen at the crack tip is indeed limited and is determined by the tensile properties; however, the scale over which the stresses act is dependent on the loading. Comparisons are good between the forward crack tip displacement and micro-fractographic measurements of "stretch" zones observed in plane strain fracture toughness tests.

17. Key Words

Stress Fields, Crack Tips,
Deformation Plasticity
Fracture Mechanics

18. Distribution Statement

Approved to Public Release Distribution Unlimited

19. Security Classif. (report)

Unclassified

20. Security Classif. (page)

Unclassified

NOMENCLATURE

c	One-half crack length
E	Young's Modulus
K	Stress intensity factor = $\bar{\sigma}\sqrt{\pi c}$
n	Strain hardening exponent
r,θ	Cylindrical coordinates measured from crack tip
T	Secant modulus = σ_e/ε_T
w_i	Displacement vector
W	Strain energy density
X	Distance in front of deformed crack tip
Y	Distance perpendicular to deformed crack tip
ε_{ij}	Strain tensor
ε_{pij}	Plastic strain tensor
ε_o	Initial yield strain
ε_p	Effective plastic strain
ε	Effective total strain
ρ	Deformed crack root radius
μ	Poisson's ratio
σ_{ij}	Stress tensor
σ_{yy}	Hoop stress
σ_e	Effective stress
σ_o	Tensile yield stress
$\bar{\sigma}$	Remote tensile stress
Φ	Airy stress function

TABLE OF CONTENTS

FIGURES

INTRODUCTION

In recent years Cherepanov [1], Rice, [2,3], Hutchinson [4,5], and Rice and Rosengren [6] have shown the asymptotic behavior of stress and strain fields surrounding sharp crack tips in plane strain. Using these studies as a guide, full field solutions with finite elements have been obtained by Levy, Marcal, Ostergren and Rice [7] and Hilton and Hutchinson [8]. These two studies give accurate near and far field behavior due to the inclusion of singular elements reflecting plasticity at the crack tip. Other numerical solutions by Marcal and King [9], Mendelson [10], Swedlow and coworkers [11,12] and Tuba [13] show qualitative features of the near field, but may not yield accurate stress field definition due to the large gradients there.

In order to have an accurate description of the near field surrounding crack tips, and hence a good understanding of the mechanisms of failure, Rice and Johnson [14] have pointed out that crack tip blunting must also be included. Their analysis accounted in an approximate manner for the blunting at the crack tip and for strain hardening in the plastic zone. As a result they showed that the stresses near the crack tip are indeed finite and that the maximum hoop stress occurred at some small distance from the deformed crack tip. A finite deformation analysis by McGowan and Smith [15] of blunted cracks in a linear (stress-strain) incompressible material shows the same general behavior. The maximum hoop stress occurs in front of the blunted crack tip and the magnitude is independent of the remote loading.

The purpose of the present study is to gain a full field solution

around a blunted crack tip in a strain hardening incompressible material under Mode I loading. This work will provide an accurate description of the stress and deformation fields immediately surrounding the blunted tip, and thereby gain insight to fracture behavior. Deformation theory of plasticity with a Mises yield condition is used. The resulting set of equations is solved for the blunted crack tip in the deformed state under load by finite differences. The linear theory of Inglis [16] gives the necessary asymptotic boundary conditions.

An initial goal of the present study was to gain a more complete understanding of the near field behavior of stress freezing photoelastic materials above critical temperature; however, this study should give considerable insight to the general behavior of engineering materials under Mode I loading.

FORMULATION OF THE PROBLEM

For small strains the compatibility equation in two dimensions is

$$\varepsilon_{11,22} + \varepsilon_{22,11} - 2\varepsilon_{12,12} = 0 \tag{1}$$

Using a deformation theory of plasticity, the constitutive equations are [10]

$$\varepsilon_{11} = \frac{1}{E}(\sigma_{11} - \mu(\sigma_{22} + \sigma_{33})) + \frac{\varepsilon_p}{\sigma_e}(\sigma_{11} - 1/2(\sigma_{22} + \sigma_{33}))$$

$$\varepsilon_{22} = \frac{1}{E}(\sigma_{22} - \mu(\sigma_{11} + \sigma_{33})) + \frac{\varepsilon_p}{\sigma_e}(\sigma_{22} - 1/2(\sigma_{11} + \sigma_{33})) \tag{2}$$

$$\varepsilon_{33} = \frac{1}{E}(\sigma_{33} - \mu(\sigma_{11} + \sigma_{22})) + \frac{\varepsilon_p}{\sigma_e}(\sigma_{33} - 1/2(\sigma_{11} + \sigma_{22}))$$

$$\varepsilon_{12} = \frac{(1+\mu)}{E}\sigma_{12} + \frac{3}{2}\frac{\varepsilon_p}{\sigma_e}\sigma_{12}$$

where

$$\sigma_e = \frac{1}{\sqrt{2}}[(\sigma_{11} - \sigma_{22})^2 + (\sigma_{22} - \sigma_{33})^2 + (\sigma_{33} - \sigma_{11})^2 + 6\sigma_{12}^2]^{1/2}$$

$$\varepsilon_p = \frac{\sqrt{2}}{3}[(\varepsilon_{p11} - \varepsilon_{p22})^2 + (\varepsilon_{p22} - \varepsilon_{p33})^2 + (\varepsilon_{p33} - \varepsilon_{p11})^2 + 6\varepsilon_{p12}^2]^{1/2} \quad (3)$$

For an incompressible material (μ=1/2) in plane strain equation (2) becomes

$$\varepsilon_{11} = \frac{3}{4}\frac{\varepsilon_T}{\sigma_e}(\sigma_{11} - \sigma_{22}) = -\varepsilon_{22}$$

$$\varepsilon_{33} = 0 \qquad \varepsilon_{12} = \frac{3}{2}\frac{\varepsilon_T}{\sigma_e}\sigma_{12} \quad (4)$$

where $\varepsilon_T = \varepsilon_p + \frac{\sigma_e}{E}$

Introducing equations (4) into the compatibility equations (1) they become

$$\frac{1}{T}(\sigma_{11,22} + \sigma_{22,11} - \sigma_{11,11} - \sigma_{22,22} - 4\sigma_{12,12})$$

$$+ 2\left(\frac{1}{T}\right)_{,2}(\sigma_{11,2} - \sigma_{22,2} - 2\sigma_{12,1}) + 2\left(\frac{1}{T}\right)_{,1}(\sigma_{22,1} - \sigma_{11,1} \quad (5)$$

$$- 2\sigma_{12,2}) + (\sigma_{11} - \sigma_{22})\left[\left(\frac{1}{T}\right)_{,22} - \left(\frac{1}{T}\right)_{,11}\right] - 4\sigma_{12}\left(\frac{1}{T}\right)_{,12} = 0$$

where T = secant modulus = σ_e/ε_T.

Introducing the Airy stress function to satisfy equilibrium

$$\sigma_{11} = \Phi_{,22} \;;\; \sigma_{22} = \Phi_{,11} \;;\; \sigma_{12} = -\Phi_{,12} \quad (6)$$

Substituting equation (6) into equation (5), the governing equation for

the field becomes

$$\frac{1}{T}(\Phi_{,2222} + \Phi_{,1111} + 2\Phi_{,1122}) + 2(\frac{1}{T})_{,1}(\Phi_{,111} + \Phi_{,122})$$

$$+ 2(\frac{1}{T})_{,2}(\Phi_{,222} + \Phi_{,112}) + (\Phi_{,22} - \Phi_{,11})[(\frac{1}{T})_{,22} - (\frac{1}{T})_{,11}] \qquad (7)$$

$$+ 4(\frac{1}{T})_{,12}\Phi_{,12} = 0$$

with

$$\varepsilon_T = \frac{1}{T}\frac{\sqrt{3}}{2}[(\Phi_{,11} - \Phi_{,22})^2 + 4\Phi_{,12}^2]^{1/2} \qquad (8)$$

For this study a Ramberg-Osgood material will be used

$$\frac{E}{\sigma_o}\varepsilon_T = \sigma_e/\sigma_o + b\alpha[(\sigma_e/\sigma_o)^{1/n} - 1]$$

$$\text{or } \frac{E}{T} = 1 + b\alpha[(\sigma_e/\sigma_o)^{(1-n)/n} - \sigma_o/\sigma_e] \qquad (9)$$

where $b = 0$ if $\sigma_e < \sigma_o$

$b = 1$ if $\sigma_e \geq \sigma_o$

Thus, the governing equation (7) will be solved subject to the constitutive laws (equations (8) and (9)).

The geometry of the blunted cracks in the deformed state under Mode I loading will resemble small elliptical perforations as shown in Figure 1. The size of the deformed crack tip root radius will be determined through integration of the strain displacement relationships

$$w_{i,j} + w_{j,i} = 2\varepsilon_{ij} \qquad (10)$$

The affected strain hardening region will be divided into a small grid utilizing elliptical coordinates and the governing set of equations will be solved through the method of finite differences. At some distance from the deformed crack tip the linear solution of Inglis [16] will

apply. The stress at the outer boundary of the inner strain hardening region will be then matched to the Inglis solution. The outer boundary will be enlarged until there is no change in the inner stress field. (A detailed description of the solution procedure is given in [17].)

PRESENTATION OF RESULTS

The stress and displacement fields in the field surrounding a deformed crack tip in a strain hardening material which is incompressible in both the elastic and plastic regions are examined. Strain hardening exponents of 0.2 through 0.01 are presented. The range of initial yield strain values is from 0.01 through 0.0001. The value of α in the effective stress-effective strain relationship, equation (9), is taken to be 1.0 in this study. (The authors have found that small changes in α and μ do not influence the solution significantly.) The "linear" results reported here are those of Inglis [16] for a deformed crack tip in a linear material. The "singular" results are those corresponding to a crack which has no root radius in a linear material.

The plastic zone shape for the smallest ellipse investigated ($\rho = 0.0018\ (K/\sigma_o)^2$) is shown in Figure 2. Note that with decreasing hardening ($n \to 0$) the plastic zone grows in maximum extent and leans progressively in the direction of crack propagation. For comparison, the singular plastic zone from McClintock and Irwin [18] and that of Levy et al [7] for a non-hardening ($n = 0$) material are also shown. As shown by Figure 2, the plastic zone shape predicted by McClintock and Irwin [18] is approached by the present study as $n \to \infty$. The difference between the plastic zone shape predicted by Levy et al [7] and the present study for $n = 0.01$ is

primarily due to the inclusion of blunting effects in the latter; the difference should be negligible as $\varepsilon_o \to 0$.

The effective stress (σ_e) is shown versus the distance ahead of the deformed crack tip in Figure 3 and the effective stress is shown versus distance perpendicular to the deformed crack tip in Figure 4. These figures show that in both cases the effective stress varies as $\frac{1}{r^{n/n+1}}$ in the plastic zone. It can be shown that the strain energy has the form:

$$\frac{2EW}{\sigma_o^2} = \left(\frac{\sigma_e}{\sigma_o}\right)^2 + \frac{2}{1+n}\, a\, b \left[\left(\frac{\sigma_e}{\sigma_o}\right)^{(1+n)/n} - 1\right]$$

Therefore, the strain energy varies approximately as 1/r in the plastic zone. This was a key assumption in the analysis of Rice and Rosengren [6] and Hutchinson [4].

The hoop stress (σ_{yy}) in front of the crack tip is shown for various values of yield strain for n = 0.2 in Figure 5, for n = 0.1 in Figure 6, and for n = 0.01 in Figure 7. As shown in these three figures, the hoop stress is substantially reduced near the crack tip because of blunting and strain hardening; with the maximum hoop stress developed forward of the crack tip. The analysis of Rice and Johnson [14] gives the same qualitative behavior; the correlation is believed to be quite reasonable in view of the several approximations involved. For a non-hardening material Rice [2] has shown that the maximum hoop stress is 2.97 σ_o. The hoop stress, as predicted by Levy et al [7], approaches this limit at the crack tip as shown in Figure 7. The hoop stress distribution of the present study in Figure 7 reflects the presence of blunting and should coincide with the work of Levy et al [7] as $\varepsilon_o \to 0$.

Figure 8 shows the variation of maximum hoop stress with initial

yield strain for varying hardening. As shown in the figure, blunting alone (linear) makes the peak hoop stress finite and the inclusion of finite deformations [15] reduces the magnitude somewhat. However, the effects of blunting and plasticity taken together are significant: the peak hoop stress is reduced by a factor of 10 from that with blunting alone. From Figure 8, one observes the peak hoop stress to be $3\sigma_0$ to $7\sigma_0$ depending upon n and σ_0/E. The peak hoop stress increases with r and decreases with σ_0/E. (The large value of peak hoop stress compared to the uniaxial yield stress, σ_0, is believed due to the presence of triaxiality in the crack tip region.)

The crack tip displacement in the direction of propagation (which is also the deformed crack root radius, ρ) is shown in Figure 9 for varying initial yield strain and hardening exponent. The present study predicts that the forward crack tip displacement increases with σ_0/E and decreases with n. For comparison one-half the crack tip opening displacement calculated by Levy et al [7] is shown. The forward crack tip displacement as predicted by the present study and the work of Levy et al [7] show parallel behavior, although they are separated by some distance. This disagreement is believed due to the shape of the crack tip being elliptical in the present study instead of cylindrical.

Included also on Figure 9 is the width of the "transition" or "stretch" zone which exists on the fracture surface between the cracked and the overload regions in fatigue. As Broek [19] has discussed, the depth of this transition zone is the crack tip opening displacement, and, therefore the width is the tip forward displacement.

Examination of the figure shows the correlation between the forward tip displacement and failure. The measurements of the stretch zone

falls close to n = 0.2. For the steels and aluminums shown values of n around 0.05 have been reported in [19], [20], and [21]. However, it is known that for this class of materials the value of n varies with plastic strain [22]. For large plastic strain (ε_p > 10%), the strain hardening exponent is close to 0.2 as shown by Jones and Brown [23] for 4340 steel. The strains in the tip region are clearly greater than 10% so that the agreement between the measurements and the analysis appears quite reasonable. The scatter band shown on the figure is an indication of the span of actual measurements (authors typically report a 40% variation).

DISCUSSION

Study of the stress fields surrounding deformed crack tips indicate that the stresses in the plastic zone will approach the $1/r^{n/n+1}$ variation as $\varepsilon_o \to 0$ as determined in the analysis of Hutchinson [4] and Rice and Rosengren [6]. However, as mentioned in the work of Levy et al [7], the J-integral may not be path independent in the plastic zone; and therefore, a full field solution is desirable in order to evaluate the strength of the stress variation in the plastic zone. For the non-hardening case, Levy et al [7] and subsequently Rice and Tracey [24] did a full field solution of a sharp crack tip utilizing singular elements. The differences in the present study and [7] and [24] is primarily due to blunting, and partially due to use here of 0.5 as an elastic Poisson's ratio. These differences should vanish as $\varepsilon_o \to 0$.

The analysis of Rice and Johnson [14] was an attempt to account for the effect of blunting near the crack tip and used the results of [4] and [6] as boundary conditions. Although approximate, the analysis of

Rice and Johnson [14] is in qualitative agreement with the present study and the stresses near the crack tip are substantially reduced. Also their analysis does predict the maximum hoop stress occurring in front of the crack tip.

Previously McGowan and Smith [15] performed a finite deformation analysis of the region surrounding deformed crack tips for a linear (stress-strain) material. The results of the finite deformation work showed that the maximum hoop stress occurred in front of the deformed crack tip also. It was determined that the stress distribution around the crack tip was "similar"; in the sense that one stress distribution could be used to describe the response of the material under load. The size of the affected zone would depend upon the load and crack length through K. The self-similarity of the stress field was a direct result of the blunting process, and would be expected to remain as long as the affected zone stayed small with respect to the crack length, thickness, or any other in-plane dimension.

The behavior is quite similar for a power hardening material. The stress field is self-similar with the size of the affected zone varying with K. The maximum hoop stress will only then be a function of the material properties E, n, and σ_0. The stretching of the similar stress distribution will depend upon K as well as the other material properties. One may conjecture that failure would depend upon the growth in size of a critical dimension such as plastic zone size which increases with K.

Wells [25] and others have used the crack opening displacement as a fracture criterion. Broek [19] has used this concept to correlate

the depth of transition zones in aluminum with fracture toughness. The present study shows good correlation of fracture toughness and transition zone width. Krafft [26], Hahn and Rosenfield [27] and Rice and Johnson [14] have all shown good correlation of plane strain fracture toughness with some minute particle size or process zone size for specific cases.

SUMMARY AND RECOMMENDATIONS

Following the pioneering studies of Hutchinson [4], Rice and Rosengren [6], Levy et al [7] and Hilton and Hutchinson [8], the authors have obtained a full field deformation plasticity finite difference solution to the Mode I plane strain problem including the effects of blunting. The material was incompressible in both the elastic and plastic regions, and followed a power hardening rule. Stress and displacement fields surrounding the deformed crack tip are presented, and are found to compare favorably both with the analysis of other investigators as well as experimental results. Because of the improved accuracy expected from a full field solution, it would be appropriate to incorporate such a solution into theories concerning void coalescence and final instability (such as the landmark studies of McClintock [28], Rice and Johnson [14] and Rice and Tracey [29]). Efforts are currently being devoted to such an approach.

ACKNOWLEDGMENTS

Much of the work done in this study was made possible by the National Science Foundation Engineering Mechanics Program under Grant No. GK-39922.

REFERENCES

[1] Cherepanov, G. P., "Crack Propagation in Continuous Media", Appl. Math. Mech. (PMM), Vol. 31, p. 476, 1967.

[2] Rice, J. R., "A Path Independent Integral and the Approximate Analysis of Strain Concentrations by Notches and Cracks", J. Appl. Mech., Vol. 35, p. 379, 1968.

[3] Rice, J. R., "Mathematical Analysis in the Mechanics of Fracture", Ch. 3 of Fracture, An Advanced Treatise, Vol. II (H. Liebowitz, ed.), Academic Press, New York, 1968.

[4] Hutchinson, J. W., "Singular Behavior at the End of a Tensile Crack in a Hardening Material", J. Mech. Phys. Solids, Vol. 16, p. 13, 1968.

[5] Hutchinson, J. W., "Plastic Stress and Strain Fields at a Crack Tip", J. Mech. Phys. Solids, Vol. 16, p. 337, 1968.

[6] Rice, J. R. and Rosengren, G. F., "Plane Strain Deformation Near a Crack Tip in a Power Law Hardening Material", J. Mech. Phys. Solids, Vol. 16, p. 1, 1968.

[7] Levy, N., Marcal, P. V., Ostergren, W. J., and Rice, J. R., "Small Scale Yielding Near a Crack in Plane Strain: A Finite Element Analysis", Int. J. Frac. Mech., Vol. 7, No. 2, p. 143, 1971.

[8] Hilton, P. D. and Hutchinson, J. W., "Plasticity Intensity Factors for Cracked Plates", Eng. Frac. Mech., Vol. 3, p. 435, 1971.

[9] Marcal, P. V. and King, I. P., "Elastic-Plastic Analysis of Two-Dimensional Stress Systems By the Finite Element Method", Int. J. Mech. Sci., Vol. 9, p. 143, 1967.

[10] Mendelson, A., Plasticity: Theory and Application, The Macmillan Company, New York, 1968.

[11] Swedlow, J. L., Yang, A. H., and Williams, M. L., "Elasto-Plastic Stresses and Strains in a Cracked Plate", in Proc. of the First Int. Conf. on Fracture, 1965, Vol. 1, p. 259, 1966.

[12] Swedlow, J. L., "Elasto-Plastic Cracked Plates in Plane Strain", Int. J. Frac. Mech., Vol. 5, p. 33, 1969.

[13] Tuba, I. S., "A Method of Elastic Plastic Plane Stress and Strain Analysis", J. of Strain Analysis, Vol. 1, p. 115, 1966.

[14] Rice, J. R. and Johnson, M. A., "The Role of Large Crack Tip Geometry Changes in Plane Strain Fracture", Inelastic Behavior of Solids (M. F. Kanninen, et al, eds.), McGraw-Hill, New York, p. 641, 1970.

[15] McGowan, J. J. and Smith, C. W., "A Finite Deformation Analysis of the Near Field Surrounding the Tip of Crack-Like Elliptical Perforations", Int. J. Frac., Vol. 11, No. 6, p. 977, 1975.

[16] Inglis, C. E., "Stresses in a Plate Due to the Presence of Cracks and Corners", Trans. Instn. Naval Archit., 55, p. 219, 1913.

[17] McGowan, J. J. and Smith, C. W., "A Finite Deformation Analysis of the Near Field Surrounding the Tip of Crack-Like Ellipses", VPI-E-74-10, May 1974.

[18] McClintock, F. A. and Irwin, G. R., "Plasticity Aspects of Fracture Mechanics", Fracture Toughness Testing and Its Applications, STP-381, ASTM p. 84, 1965.

[19] Broek, D., "Correlation Between Stretched Zone Size and Fracture Toughness", Eng. Frac. Mech., Vol. 6, No. 1, p. 173, 1974.

[20] Bates, R. C., Clark, Jr., W. G., and Moon, D. M., "Correlation of Fractographic Features with Fracture Mechanics", Electron Microfractography, STP-453, ASTM, p. 192, 1969.

[21] Pandey, R. K. and Banerjee, S., "Studies on Fracture Toughness and Fractographic Features in Fe-Mn Base Alloys", Eng. Frac. Mech., Vol. 5, No. 4, p. 965, 1973.

[22] Lauta, F. J. and Steigerwald, E. A., "Influence of Work Hardening Coefficient on Crack Propagation in High Strength Steels", AFML TR 65-31, Air Force Materials Laboratory, May 1965.

[23] Jones, M. H. and Jones, Jr., W. B., "The Influence of Crack Length and Thickness in Plane Strain Fracture Toughness Tests", Review of Developments in Plane Strain Fracture Toughness Testing, STP-463, ASTM, p. 63, 1970.

[24] Rice, J. R. and Tracey, D. M., "Computational Fracture Mechanics", Numerical and Computer Methods in Structural Mechanics (S. J. Fenves, et al, eds.), Academic Press, p. 585, 1973.

[25] Wells, A. A., "Crack Opening Displacements from Elastic-Plastic Analyses of Externally Notched Tension Bars", Eng. Frac. Mech., Vol. 1, No. 3, p. 399, 1969.

[26] Krafft, J., "Correlation of Plane Strain Crack Toughness with Strain Hardening Chracteristics of a Low, a Medium, and a High Strength Steel", Applied Material Research, Vol. 3, p. 1964, 1964.

[27] Hahn, G. and Rosenfield, A., "Source of Fracture Toughness: The Relation Between K_{Ic} and the Ordinary Tensile Properties of Metals", Applications Related Phenomena in Titanium Alloys, STP-432, ASTM, p. 5, 1968.

[28] McClintock, F. A., "A Criterion for Ductile Fracture by the Growth of Holes", J. Appl. Mech., Vol. 35, p. 363, 1968.

[29] Rice, J. R. and Tracey, D. M., "On the Ductile Enlargement of Voids in Triaxial Stress Fields", J. Mech. Phys. Solids, Vol. 17, p. 201, 1969.

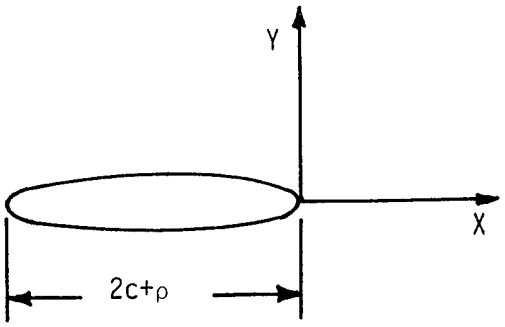

Deformed crack geometry

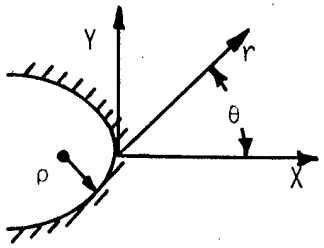

Enlarged view of deformed crack tip region

Figure 1 Problem geometry

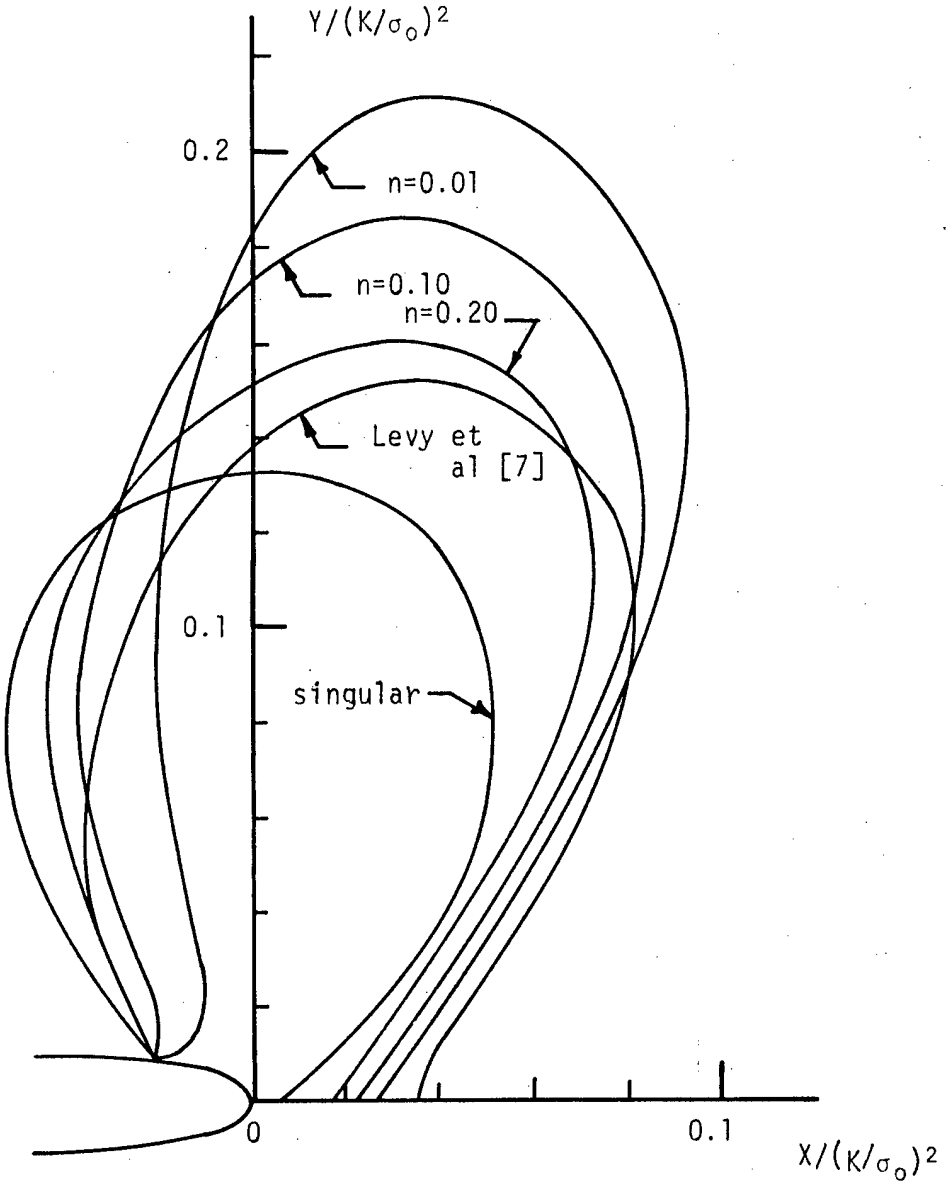

Figure 2 Plastic zone shape for the blunted crack for several strain hardening exponents with a deformed root radius of $\rho=0.0018(K/\sigma_o)^2$.

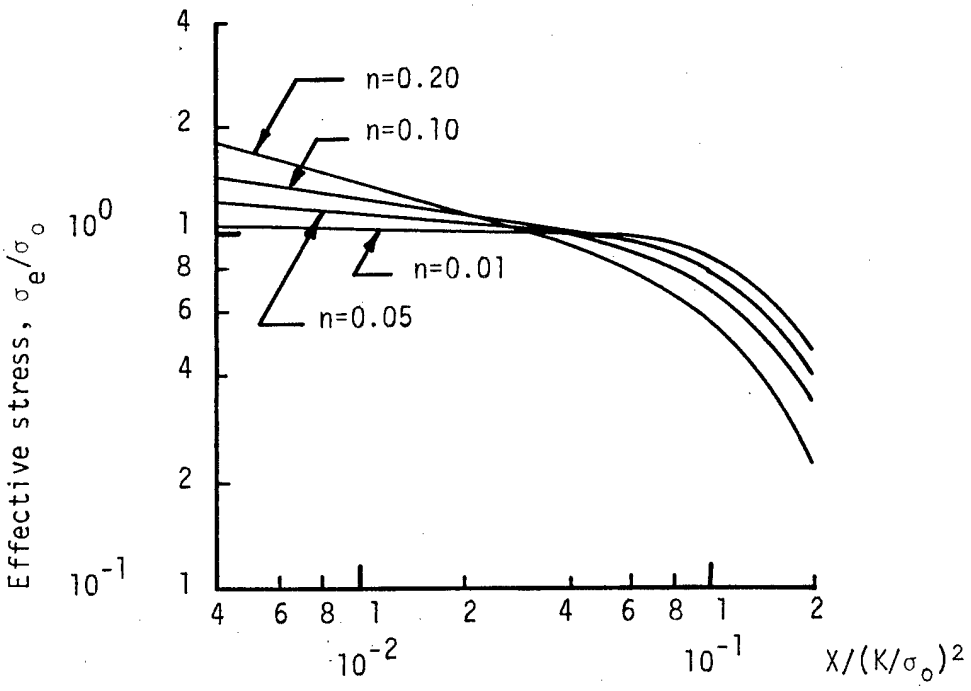

Figure 3 Effective stress distribution forward of the blunted crack tip for several strain hardening exponents with a crack root radius of $\rho=0.0018$ $(K/\sigma_o)^2$.

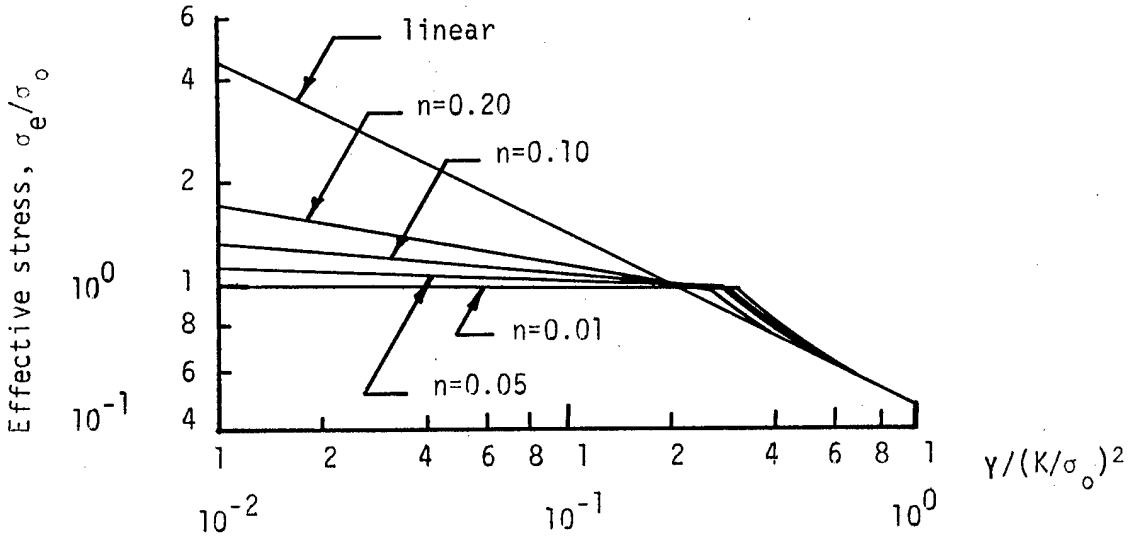

Figure 4 Effective stress distribution perpendicular to the blunted crack tip for several strain hardening exponents with a crack root radius of $\rho=0.0018$ $(K/\sigma_o)^2$.

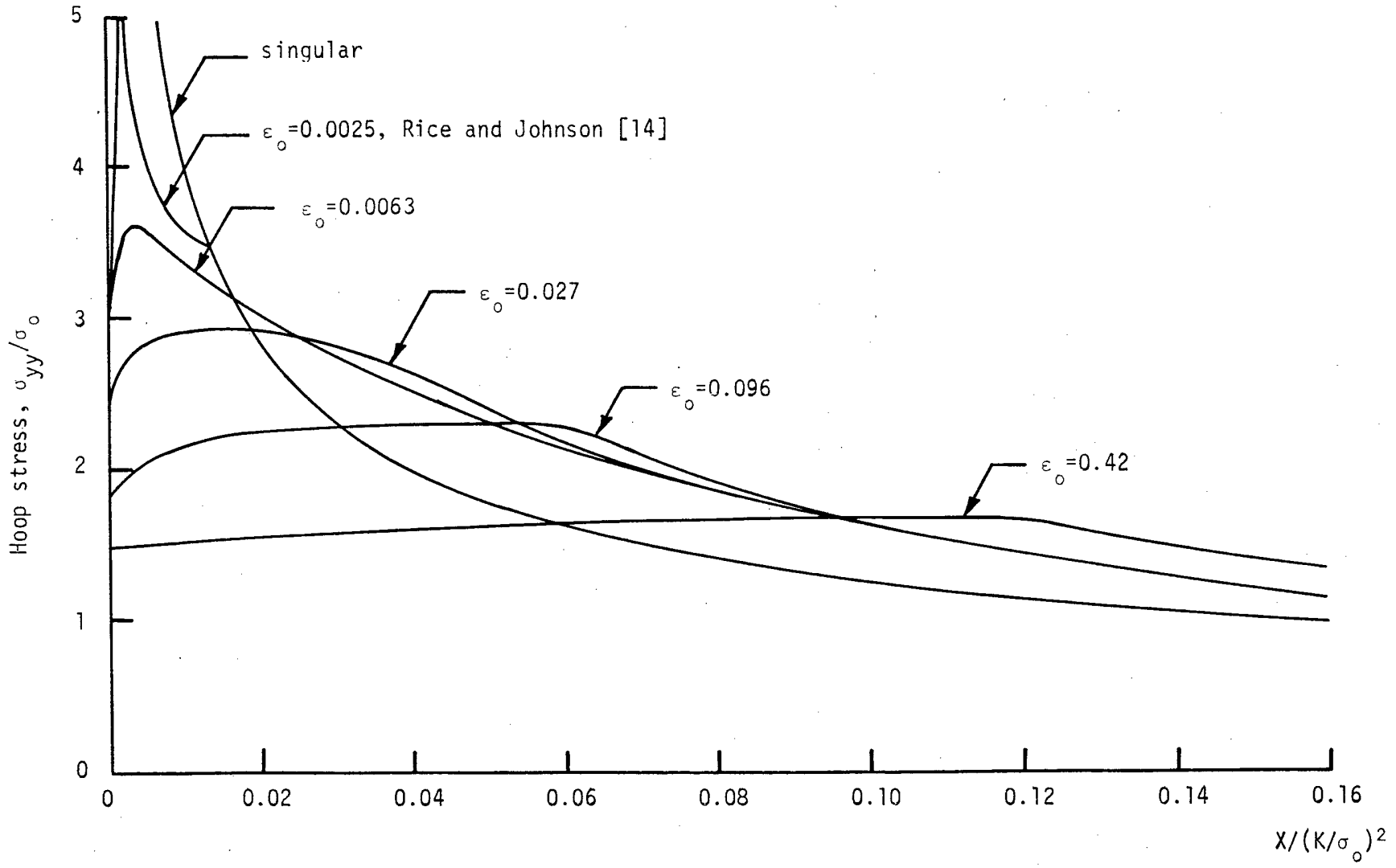

Figure 5 Hoop stress distribution forward of the blunted crack tip for several values of initial yield strain with a strain hardening exponent of n=0.20.

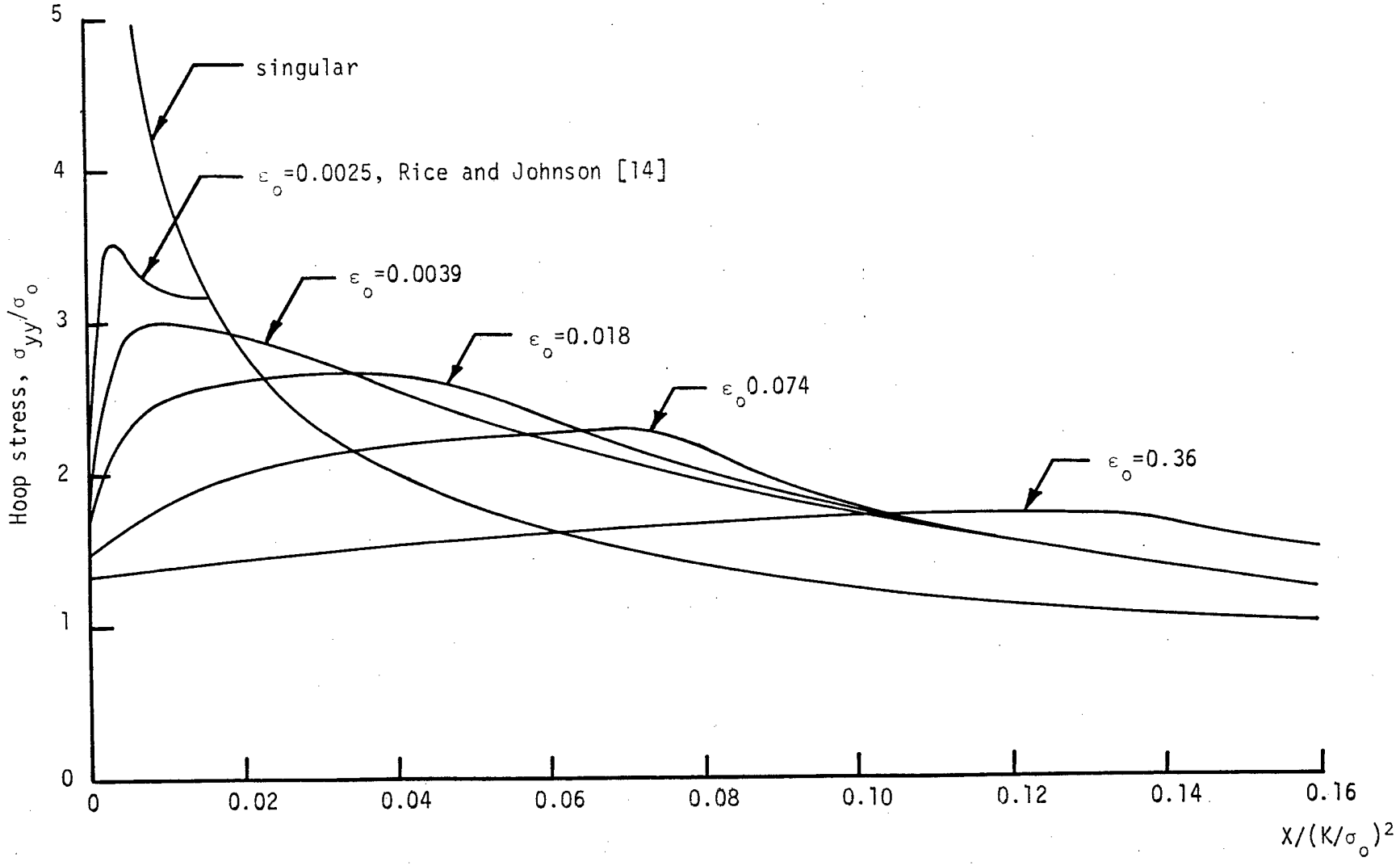

Figure 6 Hoop stress distribution forward of the blunted crack tip for several values of initial yield strain with a strain hardening exponent of n=0.10.

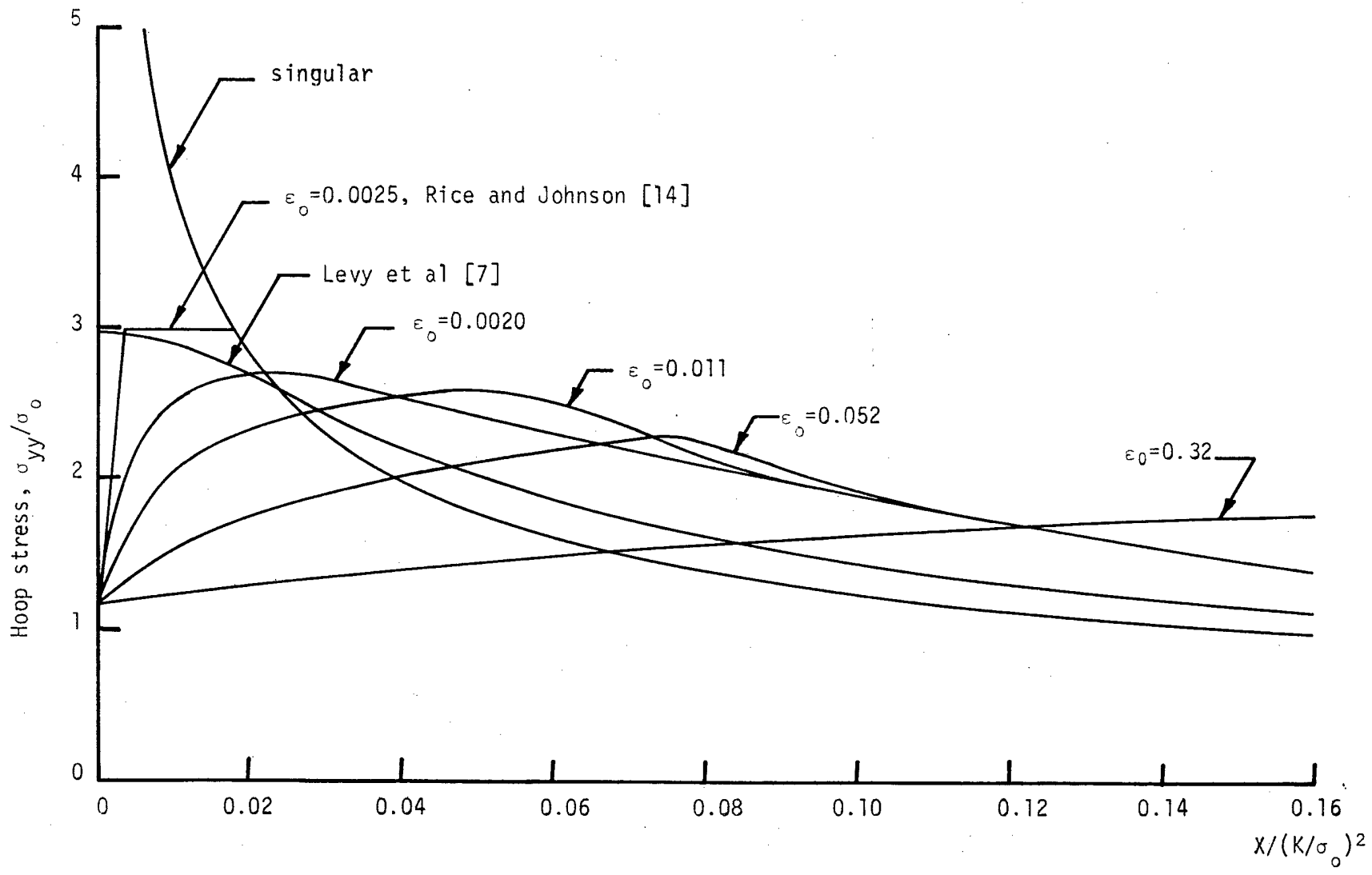

Figure 7 Hoop stress distribution forward of the blunted crack tip for several values of initial yield strain with a strain hardening exponent of n=0.01.

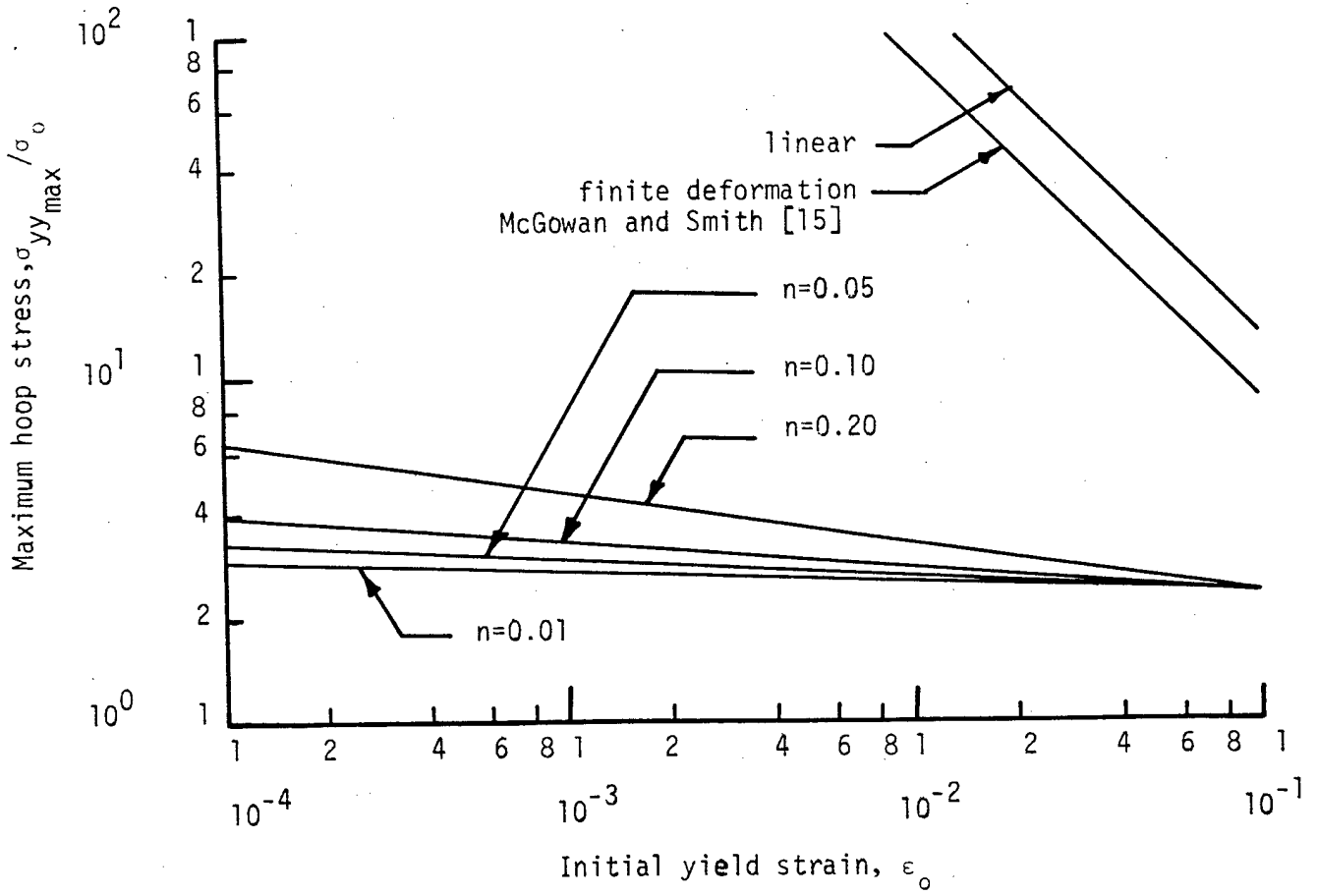

Figure 8 Variation of hoop stress maximum with initial yield strain for several values of strain hardening exponent.

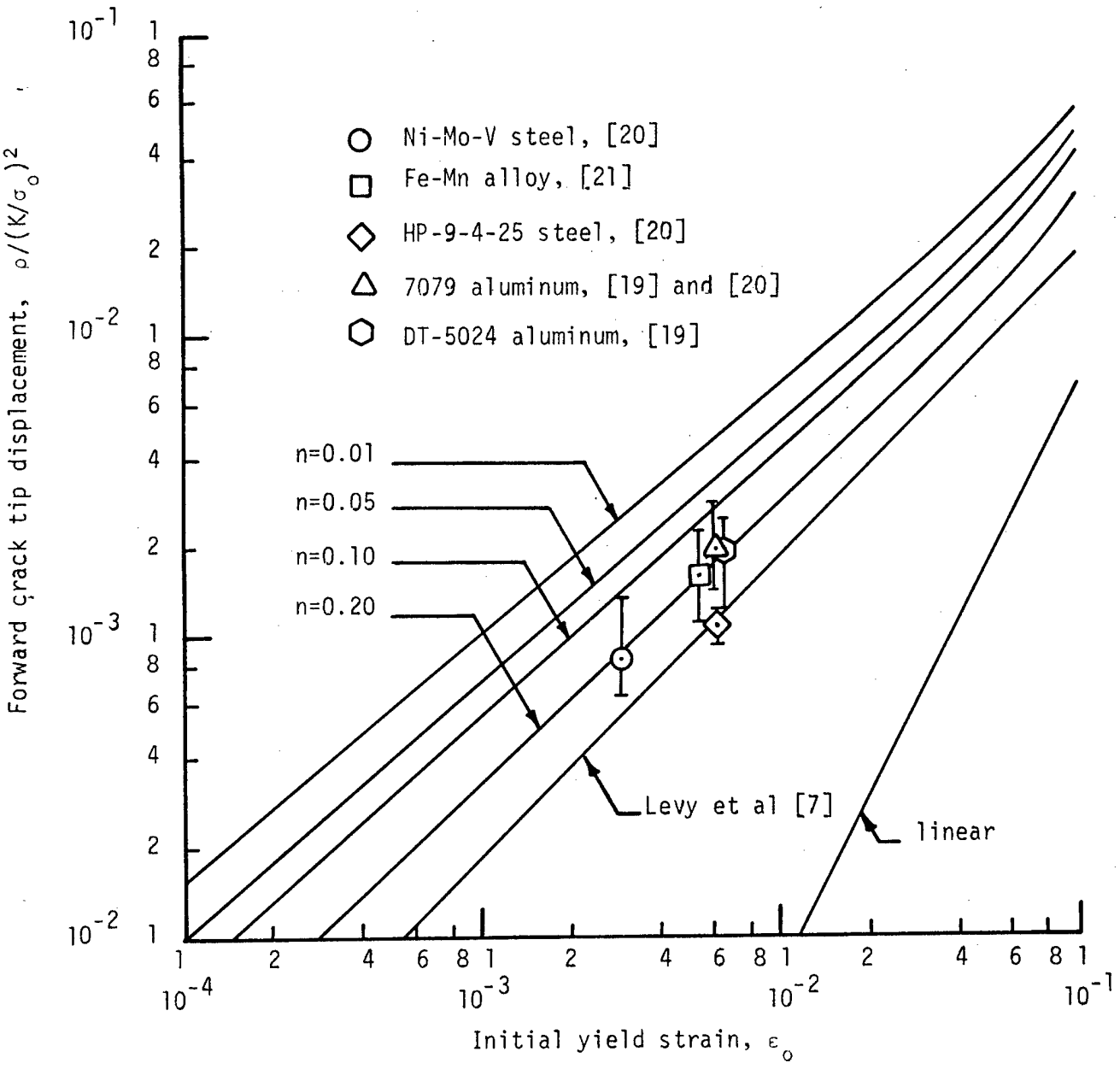

Figure 9 Forward crack tip displacement variation with initial yield strain for several values of strain hardening exponent. Also shown are experimental measurements of 'stretch' zones in various steels and aluminums.